Supporting Information

Doped TiO_2-Supported IrO_2 Electrocatalyst with High Activity and Durability toward the Acidic Oxygen Evolution Reaction

Zhen Fang,[†a,e] Zhongmin Tang,[†*b] Senming Lin,[b] Runhua Li,[a,e] Xiaomei Chen,[b] Jiakang Tian,[a,e] Lijiang Liu,[b] Jiaheng Peng,[*a,e] Shuai Liu,[b] Benwei Fu,[a] Tao Deng,[*a,c] and Jianbo Wu[*a,c,d,e]

[a]*State Key Laboratory of Metal Matrix Composites, School of Materials Science and Engineering, Shanghai Jiao Tong University, Shanghai 200240, P. R. China.*
E-mail:
jianbowu@sjtu.edu.cn
dengtao@sjtu.edu.cn
pengjiaheng_2016@sjtu.edu.cn

[b]*Emergency Rescue Center of Xinjiang Oilfield Company.*
E-mail:
yjjytangzm@petrochina.com.cn

Characterization data

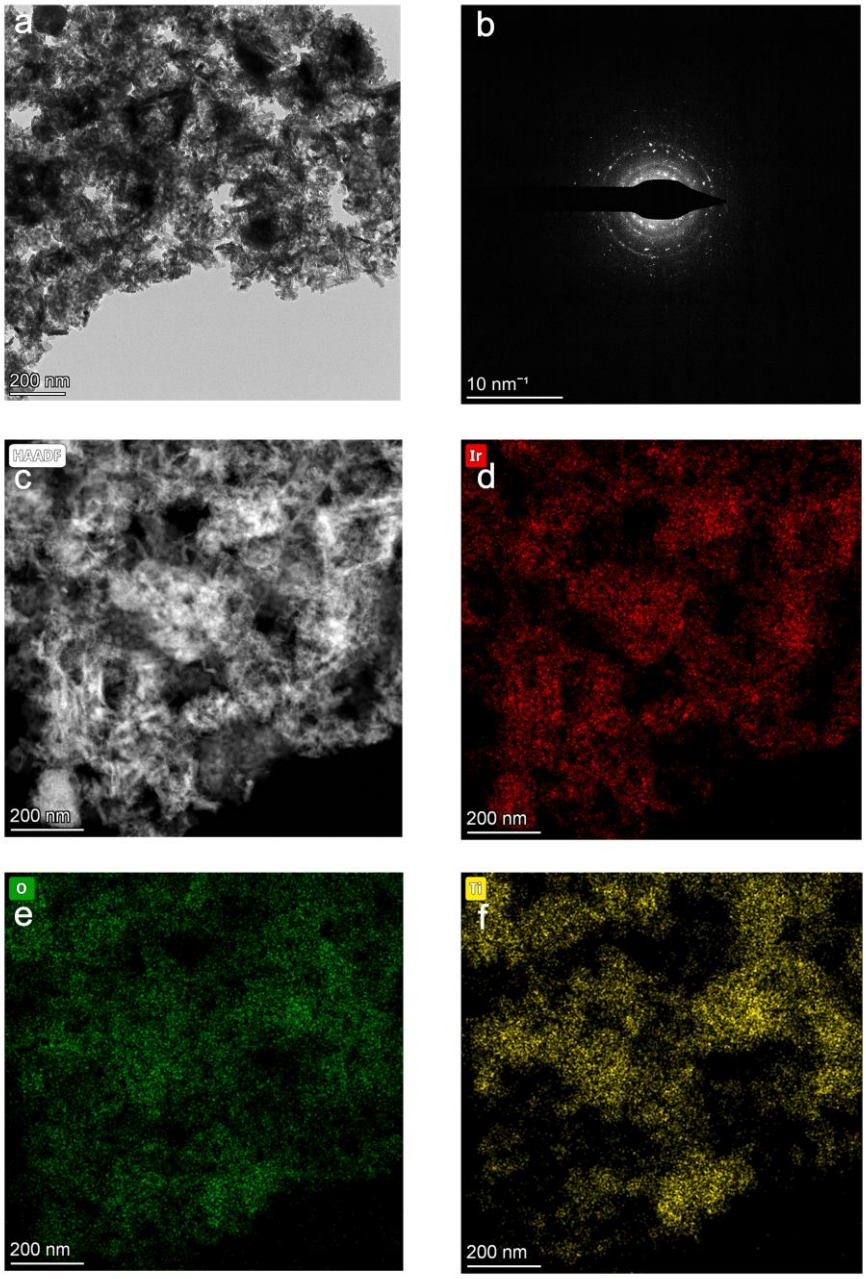

Figure S1. TEM images, SAED patterns, HAADF-STEM images and EDS elemental mappings of TiO_2@IrO_2.

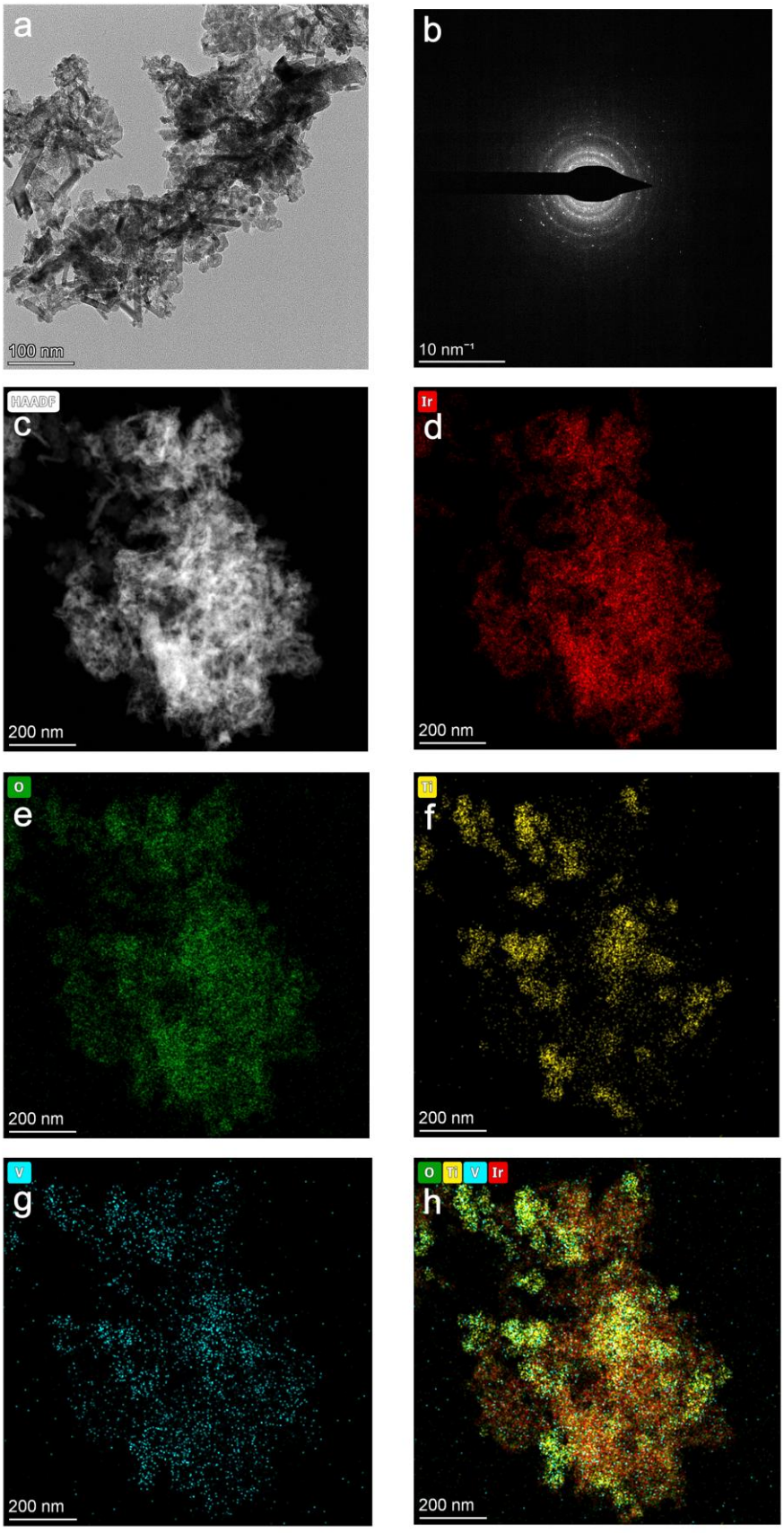

Figure S2. TEM images, SAED patterns, HAADF-STEM images and EDS elemental mappings of V-TiO_2@IrO_2.

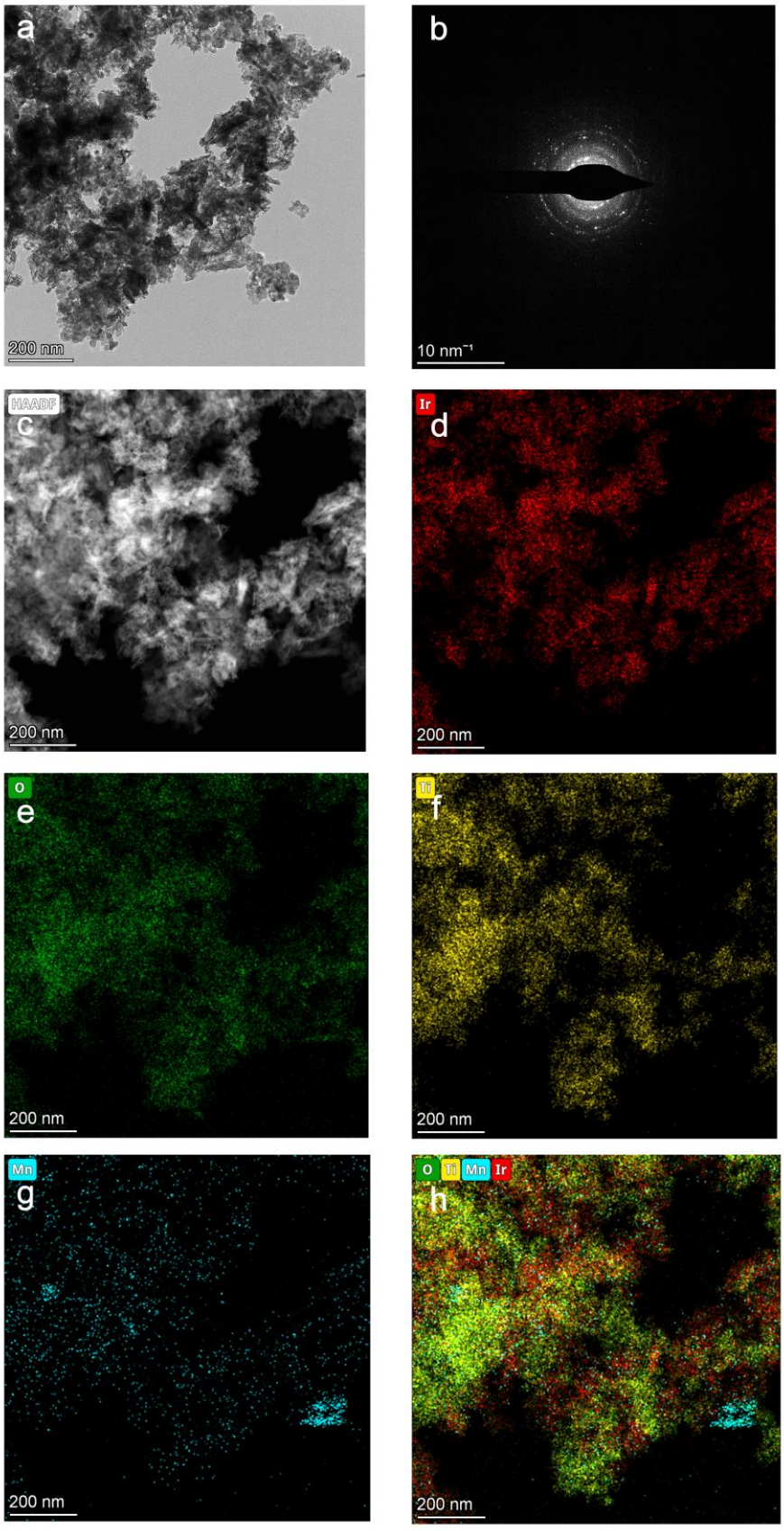

Figure S3. TEM images, SAED patterns, HAADF-STEM images and EDS elemental mappings of Mn-TiO_2@IrO_2.

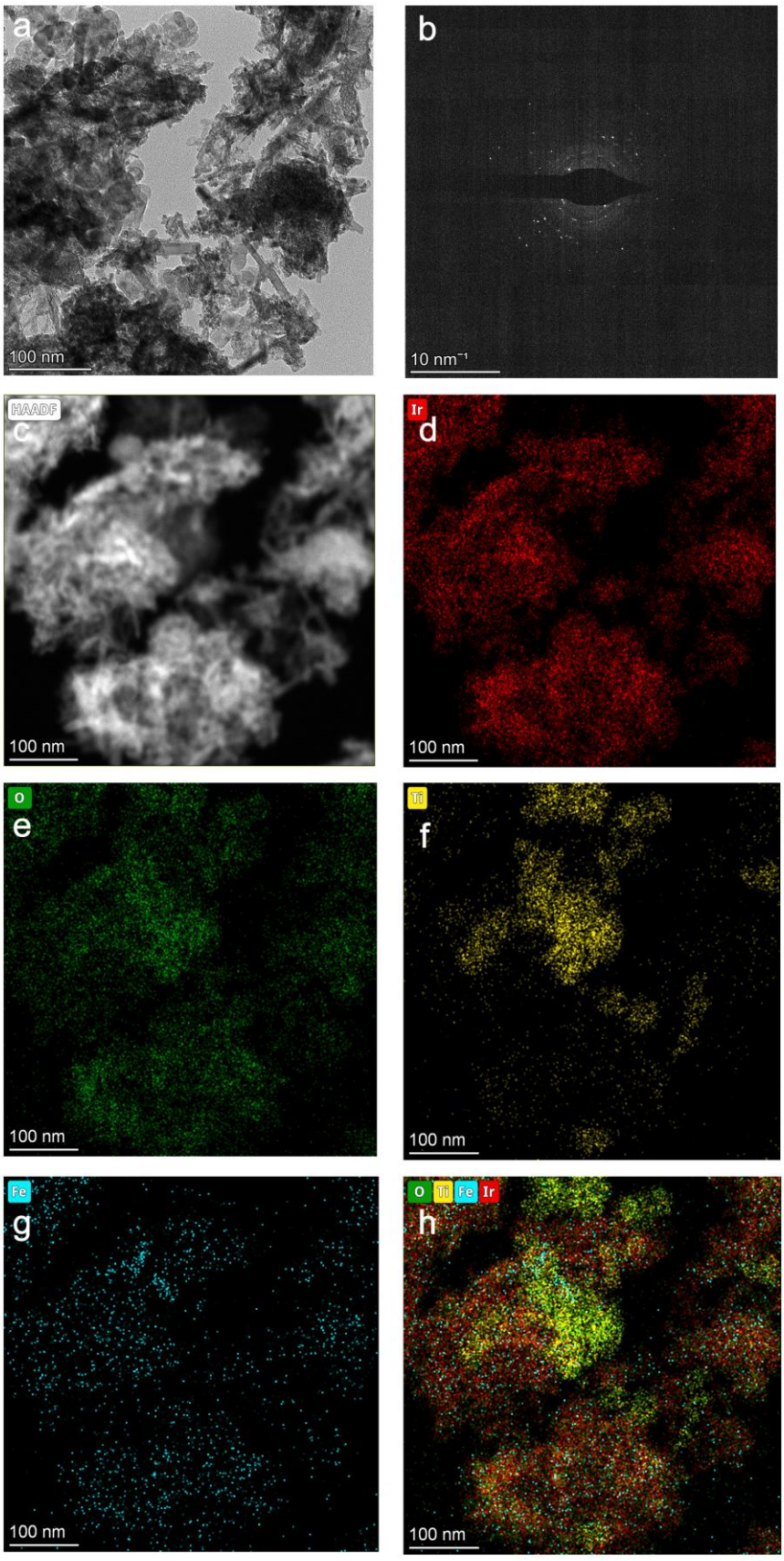

Figure S4. TEM images, SAED patterns, HAADF-STEM images and EDS elemental mappings of Fe-TiO_2@IrO_2.

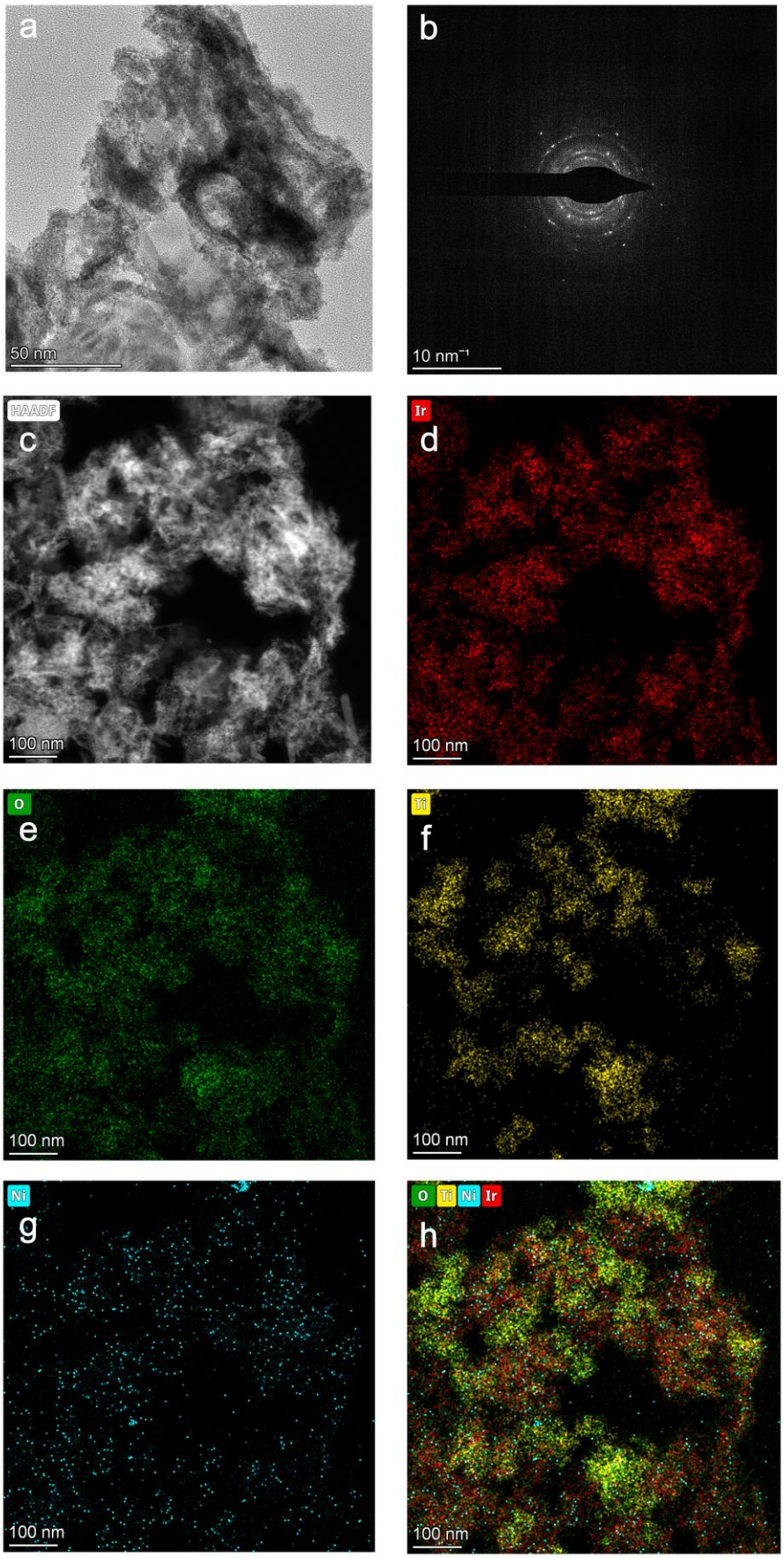

Figure S5. TEM images, SAED patterns, HAADF-STEM images and EDS elemental mappings of Ni-TiO_2@IrO_2.

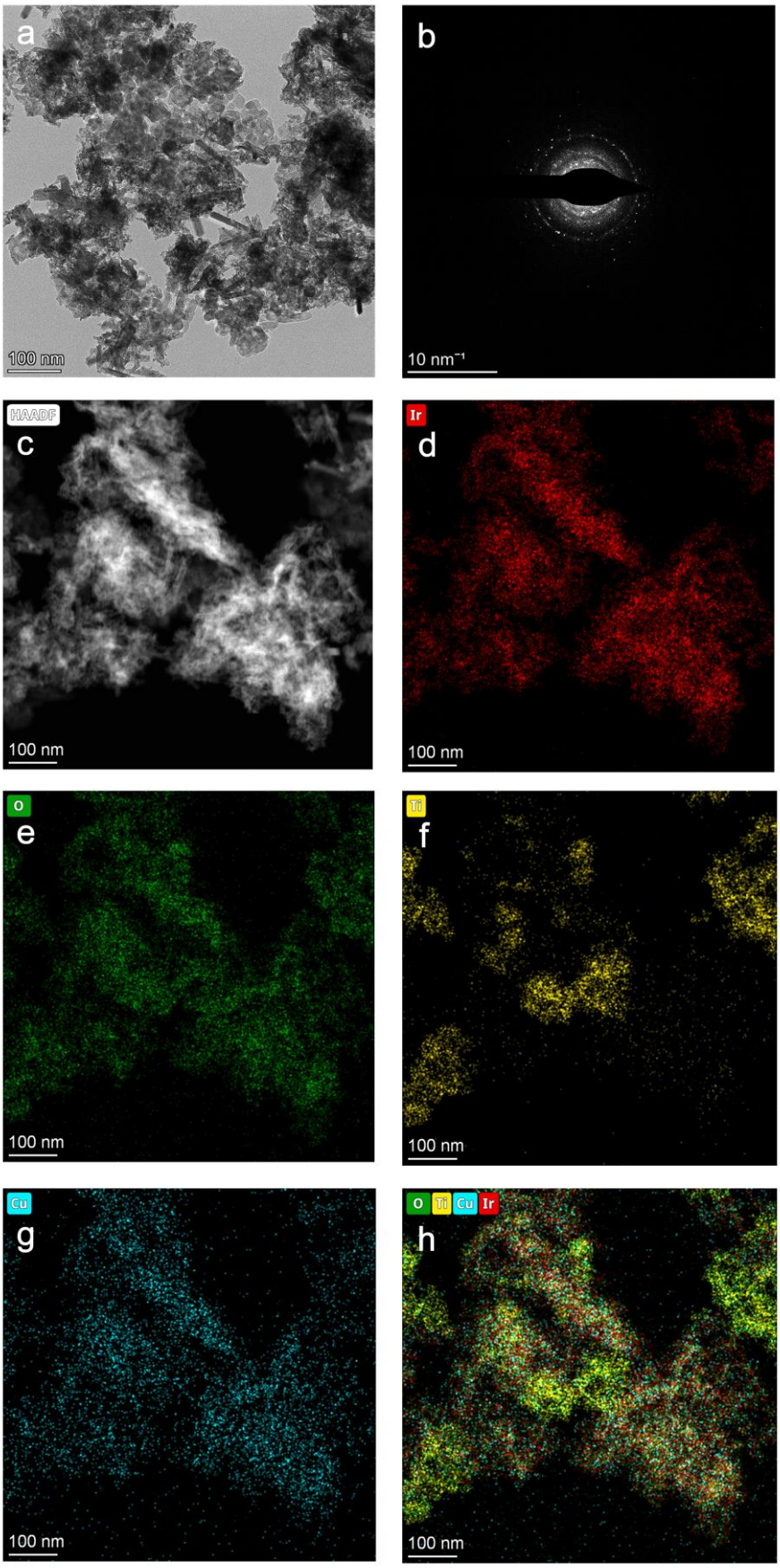

Figure S6. TEM images, SAED patterns, HAADF-STEM images and EDS elemental mappings of Cu-TiO_2@IrO_2.

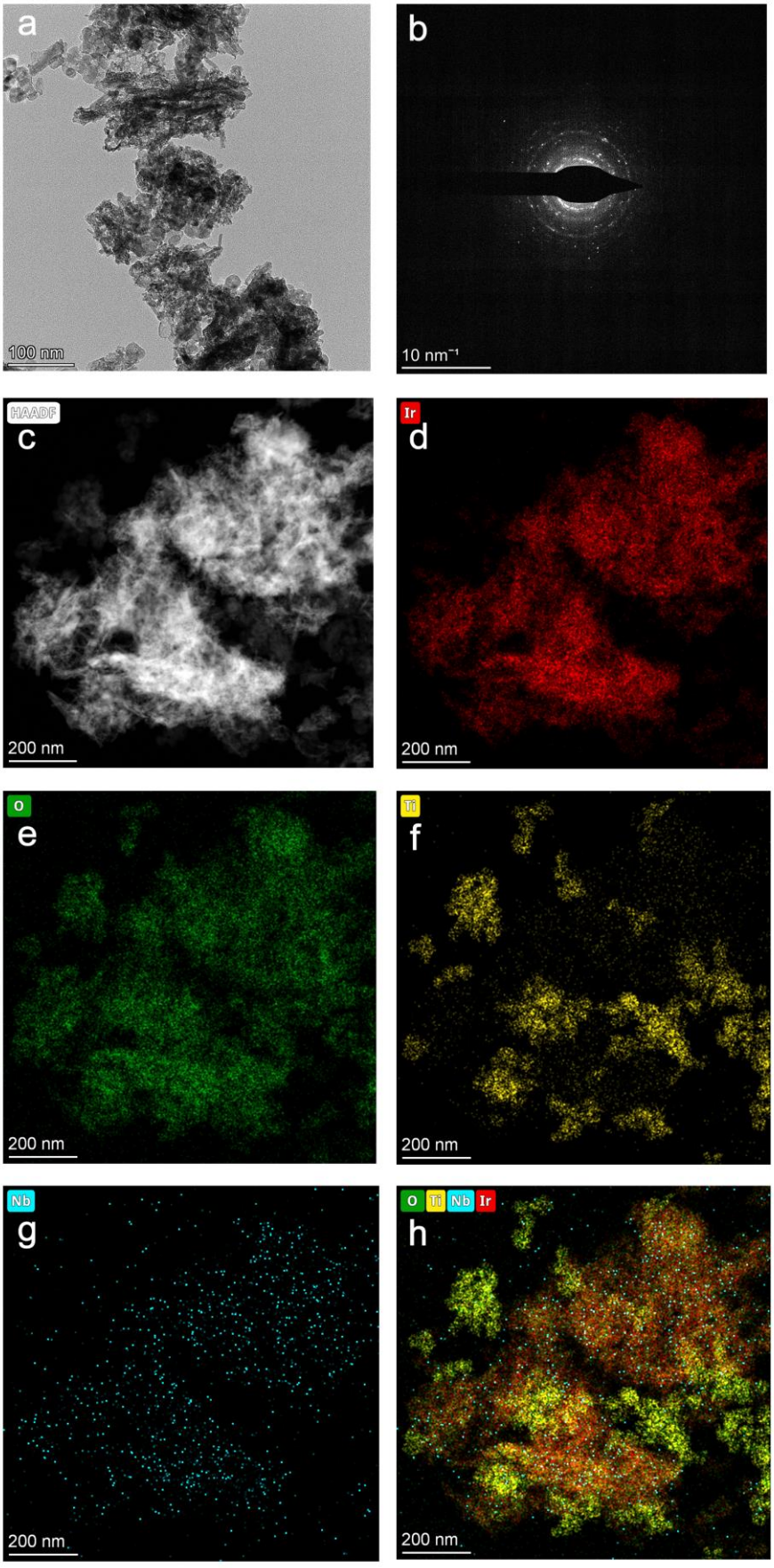

Figure S7. TEM images, SAED patterns, HAADF-STEM images and EDS elemental mappings of Nb-TiO_2@IrO_2.

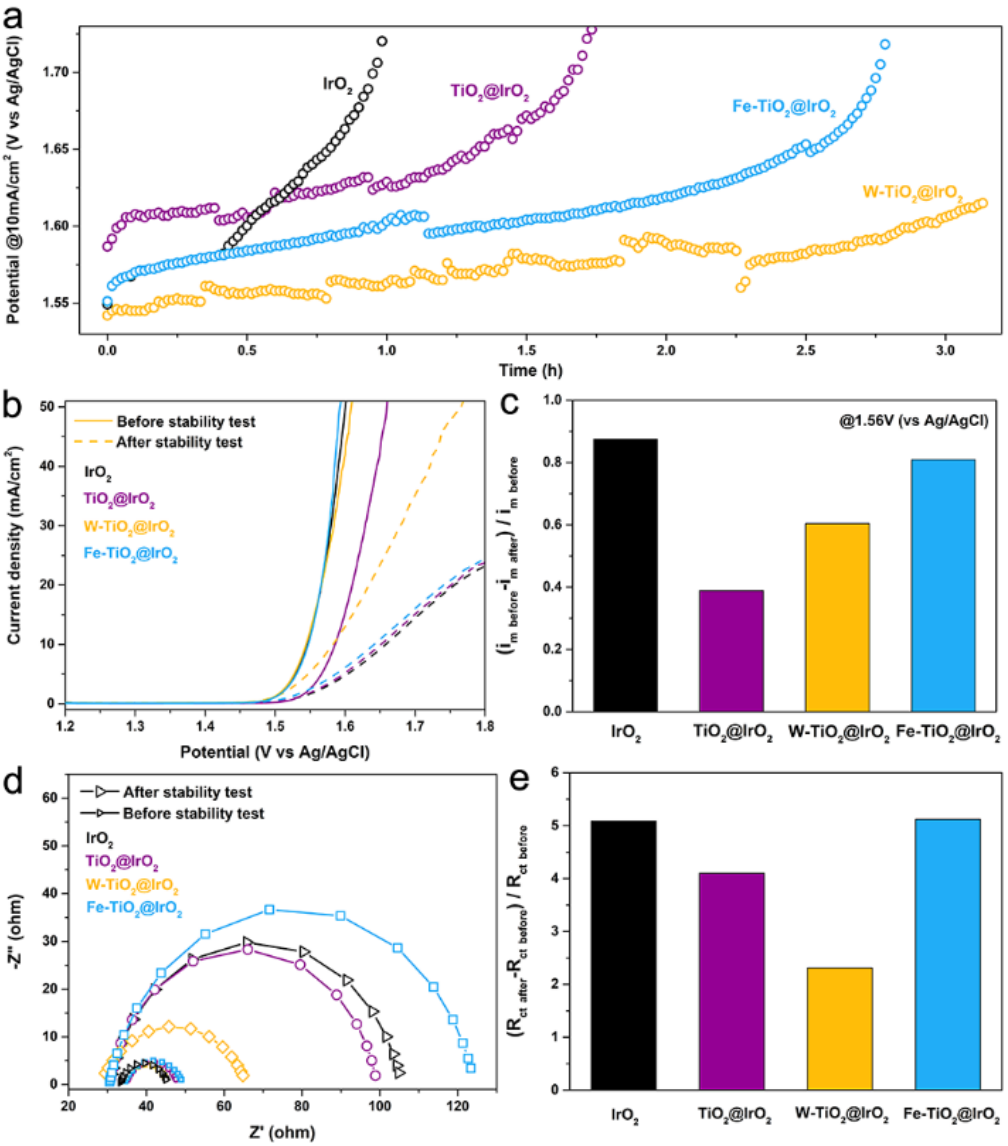

Figure S8. Electrocatalysis OER stability test of unsupported IrO_2, TiO_2@IrO_2, Fe-TiO_2@IrO_2, and W-TiO_2@IrO_2 (test lasting for 3.1h). (a) Chronopotentiometry test at 10mA/cm^2_{geo}. (b) OER activity before and after the chronopotentiometry test. (c) The attenuation degree of mass activity (i_m) before and after the chronopotentiometry test at 1.56 V (vs Ag/AgCl). (d) Nyquist plots before and after chronopotentiometry test at the potential of 10 mA/cm^2_{geo}. (e) The increased degree of R_{ct} before and after the chronopotentiometry test corresponding to the Nyquist plots.

Table S1. Performance table of Ir-based electrocatalysts.

Catalyst	Electrolyte	Overpotential @10mA/cm^2(mV)	Tafel slope (mV/dec)	Mass activity (A/mg$_{Ir}$) @Overpotential (V)	Ref.
W-TiO_2/IrO_2	0.1M $HClO_4$	308	42.36	0.72@330	This work
IrO_2	0.1M $HClO_4$	373	112	0.0126@300	[1]
IrO_2 ns	0.5M H_2SO_4	350	57	0.437@xx	[2]
Ni&Co-IrO_2	0.1M $HClO_4$	~280	53	0.055@270	[3]
TiO_2/IrO_2	0.1M $HClO_4$	255@1mA/cm^2	42	0.07@295	[4]
Nb-TiO_2/IrO_2	0.1M $HClO_4$	310	/	/	[5]
$Nb_{0.05}TiO_{0.95}O_2$/IrO_2	0.5M H_2SO_4	270@1mA/cm^2	282	0.471@370	[6]
$W_xTi_{1-x}O_2$/Ir	0.1M $HClO_4$	~300	/	~0.77@570	[7]
TiN/IrO_2	0.5M H_2SO_4	313	65.5	0.874@370	[8]
IrNiCu DNF/C	0.1M $HClO_4$	307	48	0.053@300	[9]
IrCoNi PHNCs	0.1M $HClO_4$	303	53.8	0.7@300	[10]
P-$IrCu_{1.4}$NCs	0.05M H_2SO_4	311	53.9	0.213@320	[11]
$SrCo_{0.9}Ir_{0.1}O_{3-\sigma}$	0.1M $HClO_4$	310	/	/	[12]
RuIr	0.1M $HClO_4$	344	111.5	/	[13]
IrOOH NSs	0.1M $HClO_4$	344	58	/	[14]
Sputtered IrO_x films	0.1M $HClO_4$	490	100	/	[15]

[1] Wu G, Zheng X, Cui P, et al. A general synthesis approach for amorphous noble metal nanosheets. Nature Communications, 2019, 10(1): 4855.

[2] Takimoto D, Ayato Y, Mochizuki D, et al. Lateral Size Effects of Two-dimensional IrO_2 Nanosheets towards the Oxygen Evolution Reaction Activity. Electrochemistry, 2017, 85(12): 779-783.

[3] Zaman W Q, Wang Z, Sun W, et al. Ni–Co codoping breaks the limitation of single-metal-doped IrO_2 with higher oxygen evolution reaction performance and less iridium. ACS Energy Letters, 2017, 2(12): 2786-2793.

[4] Oakton E, Lebedev D, Povia M, et al. IrO_2-TiO_2: A high-surface-area, active, and stable electrocatalyst for the oxygen evolution reaction. ACS Catalysis, 2017, 7(4): 2346-2352.

[5] Hao C, Lv H, Mi C, et al. Investigation of mesoporous niobium-doped TiO_2 as an oxygen evolution catalyst support in an SPE water electrolyzer. ACS Sustainable Chemistry & Engineering, 2016, 4(3): 746-756.

[6] Hu W, Chen S, Xia Q. IrO_2/Nb–TiO_2 electrocatalyst for oxygen evolution reaction in acidic medium. International journal of hydrogen energy, 2014, 39(13): 6967-6976.

[7] Zhao S, Stocks A, Rasimick B, et al. Highly active, durable dispersed iridium nanocatalysts for PEM water electrolyzers. Journal of the Electrochemical Society, 2018, 165(2): F82.

[8] Zhang K, Mai W, Li J, et al. Highly scattered Ir oxides on TiN as an efficient oxygen evolution reaction electrocatalyst in acidic media. Journal of Materials Science, 2020, 55: 3507-3520.

[9] Lim J, Park D, Jeon S S, et al. Ultrathin IrO_2 nanoneedles for electrochemical water oxidation. Advanced Functional Materials, 2018, 28(4): 1704796.

[10] Feng J, Lv F, Zhang W, et al. Iridium-based multimetallic porous hollow nanocrystals for efficient overall-water-splitting catalysis. Advanced Materials, 2017, 29(47): 1703798.

[11] Pi Y, Guo J, Shao Q, et al. Highly efficient acidic oxygen evolution electrocatalysis enabled by porous Ir–Cu nanocrystals with three-dimensional electrocatalytic surfaces. Chemistry of Materials, 2018, 30(23): 8571-8578.

[12] Chen Y, Li H, Wang J, et al. Exceptionally active iridium evolved from a pseudo-cubic perovskite for oxygen evolution in acid. Nature Communications, 2019, 10(1): 572.
[13] Shan J, Ling T, Davey K, et al. Transition-metal-doped RuIr bifunctional nanocrystals for overall water splitting in acidic environments. Advanced Materials, 2019, 31(17): 1900510.
[14] Weber D, Schoop L M, Wurmbrand D, et al. IrOOH nanosheets as acid stable electrocatalysts for the oxygen evolution reaction. Journal of Materials Chemistry A, 2018, 6(43): 21558-21566.
[15] Baker D R, Graziano M B, Hanrahan B M. Nanostructured antireflective iridium oxide coating for water oxidation. The Journal of Physical Chemistry C, 2018, 122(23): 12207-12214.